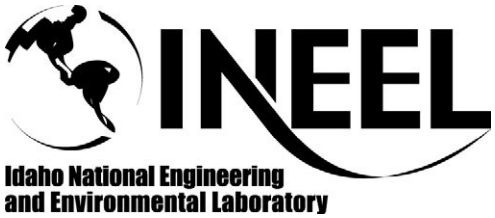

INEEL/CON-03-00995
PREPRINT

The Addition Of Noncondensable Gases Into RELAP5-3D For Analysis Of High Temperature Gas-Cooled Reactors

C. B. Davis
C. H. Oh

August 27, 2003

2003 RELAP5 International Users Seminar

2003 RELAP5 International Users Seminar
West Yellowstone, Montana
August 27-29, 2003

THE ADDITION OF NONCONDENSABLE GASES INTO RELAP5-3D FOR ANALYSIS OF HIGH TEMPERATURE GAS-COOLED REACTORS

C. B. Davis
C. H. Oh

Idaho National Engineering and Environmental Laboratory
P. O. Box 1625
Idaho Falls, ID 83415-3890

ABSTRACT

Oxygen, carbon dioxide, and carbon monoxide have been added to the RELAP5-3D computer code as noncondensable gases to support analysis of high temperature gas-cooled reactors. Models of these gases are required to simulate the effects of air ingress on graphite oxidation following a loss-of-coolant accident. Correlations were developed for specific internal energy, thermal conductivity, and viscosity for each gas at temperatures up to 3000 K. The existing model for internal energy (a quadratic function of temperature) was not sufficiently accurate at these high temperatures and was replaced by a more general, fourth-order polynomial. The maximum deviation between the correlations and the underlying data was 2.2% for the specific internal energy and 7% for the specific heat capacity at constant volume. The maximum deviation in the transport properties was 4% for oxygen and carbon monoxide and 12% for carbon dioxide.

INTRODUCTION

A very high temperature gas-cooled reactor is being evaluated in the Department of Energy's Generation IV reactor program. The current design utilizes helium as the reactor coolant and graphite in the fuel blocks and reflectors (Oh et al. 2002). The graphite can oxidize due to air ingress that can follow a loss-of-coolant accident. The reaction between the oxygen in the air and graphite results in the formation of carbon dioxide and carbon monoxide. A graphite oxidation model (Siefken et al. 2002) has been incorporated into RELAP5-3D code (RELAP5-3D Development Team 2002). The temperature range of interest for graphite oxidation is from 395 to 2073 K. This report documents the addition of oxygen, carbon dioxide,[1] and carbon monoxide noncondensable gases into RELAP5.

RELAP5 currently contains models for several noncondensable gases, including helium, hydrogen, nitrogen, krypton, xenon, air, and argon. The code assumes that each noncondensable species is an ideal gas whose density is determined by the ideal gas law. Furthermore, the internal energy is assumed to be a function of temperature alone. The inclusion of a noncondensable species into RELAP5 requires a gas constant, correlations for the internal energy,

[1] RELAP5 currently models carbon dioxide as a working fluid, with a complete equation of state for the liquid and gas phases. However, the working fluid in a very high temperature gas reactor is helium, which requires that carbon dioxide also be simulated as a noncondensable.

thermal conductivity, viscosity, and diffusion coefficients. The remainder of this paper describes the development of these parameters, conclusions and references.

REQUIRED NONCONDENSABLE PARAMETERS

The following subsections describe the parameters needed for each noncondensable gas, including the gas constant, correlations for specific internal energy, thermal conductivity, and viscosity, and diffusion parameters.

Gas Constants

The gas constant for each species, R_{ni}, of noncondensable gas is calculated as

$$R_{ni} = \frac{R}{M_{ni}} \tag{1}$$

where R is the universal gas constant (8314.3 J/kg-K) and M_{ni} is the molecular weight. Table 1 shows the molecular weight and gas constant for each species. These values were obtained from Appendix C of Zucrow and Hoffman (1976).

Table 1. Gas constants.

Species	**M_{ni}**	**R_{ni} (J/kg-K)**
Oxygen	32.000	8,314.3/32.000 = 259.82
Carbon dioxide	44.010	8,314.3/44.010 = 188.92
Carbon monoxide	28.010	8,314.3/28.010 = 296.83

Specific Internal Energy

RELAP5-3D assumes that the specific internal energy of a noncondensable species, U_{ni}, is (see Equation 3.2-26 of Volume 1 of the code manual (RELAP5-3D Development Team 2002))

$$U_{ni} = U_{o,ni} + C_{o,ni}T \qquad \text{for } T < T_o \tag{2}$$

$$U_{ni} = U_{o,ni} + C_{o,ni}T + 0.5D_{o,ni}(T - T_o)^2 \qquad \text{for } T > T_o \tag{3}$$

where $U_{o,ni}$, $C_{o,ni}$, and $D_{o,ni}$ are constants that vary between species, T is the temperature in degrees Kelvin, and T_o = 250 K. $U_{o,ni}$ and $D_{o,ni}$ were obtained by least-squares fitting to the data reported by Reynolds (1979) for 250 < T < 700 K for the currently modeled noncondensable gases. For monatomic gases, such as helium and xenon, $C_{o,ni}$ is set to 1.5 R_{ni} . For diatomic gases, such as hydrogen and nitrogen, $C_{o,ni}$ is set to 2.5 R_{ni}.

Differentiating Equations (2) and (3) with respect to temperature yields the specific heat capacity at constant volume, $C_{v,ni}$,

$$C_{v,ni} = C_{o,ni} \qquad \text{for } T < T_o \tag{4}$$

$$C_{v,ni} = C_{o,ni} + D_{o,ni}(T - T_o) \qquad \text{for } T > T_o \tag{5}$$

Equations (4) and (5) show that $C_{v,ni}$ is assumed to be constant at low temperatures and linear at higher temperatures. The linear assumption is reasonable for the temperature range between 250 and 700 K, but is not sufficiently accurate when the temperatures are extended to near 2000 K. Consequently, the functional form of the specific internal energy in Equation (3) was changed to

$$U_{ni} = U_{o,ni} + C_{o,ni}T + D_{o,ni}(T - T_o)^2/2 + E_{o,ni}(T - T_o)^3/3 + F_{o,ni}(T - T_o)^4/4 \quad \text{for } T > T_o \quad (6)$$

The values of the constants were determined by the method of least squares using values from Rivken (1988) for temperatures between 250 and 289 K and from Avallone (1987) for temperatures between 289 and 3000 K. The values of the coefficients are shown in Table 2. The fitted values of $C_{o,ni} / R_{ni}$ are 2.46 for oxygen and 2.34 for carbon monoxide, which are close to the 2.5 value derived from kinetic theory for rigid diatomic molecules (Zucrow and Hoffman 1976). The fitted value of $C_{o,ni} / R_{ni}$ for carbon dioxide is 3.49, which is reasonably close to the theoretical value of 3.0 for rigid polyatomic molecules.

Table 2. Specific internal energy coefficients.

Gas species	**$U_{o,ni}$ (J/kg)**	**$C_{o,ni}$ (J/kg-K)**	**$D_{o,ni}$ (J/kg-K^2)**	**$E_{o,ni}$ (J/kg-K^3)**	**$F_{o,ni}$ (J/kg-K^4)**
Oxygen	1,641.42	639.8541	0.3537302	-1.613807e-4	2.923424e-8
Carbon dioxide	-41,467.2	658.7377	0.7563373	-3.726885e-4	6.513268e-8
Carbon monoxide	14,231.1	693.2758	0.3421647	-1.216078e-4	1.503636e-8

Figure 1 compares the results of Equation (6) with the constants from Table 2 and the spliced values reported by Rivken (1988) and Avallone (1987) for oxygen. The results are in excellent agreement with a maximum deviation of 0.7%. Figure 2 compares the specific heat capacity at constant volume, C_v, which is obtained by differentiating Equation (6) with respect to temperature, for oxygen to reported results from a variety of sources, including Avalone (1987), Rivken (1988), Lemmon et al. (2002), Kayes and Crawford (1980), and Reynolds (1979). The fitted results are generally in excellent agreement. However, the fitted results diverge slightly at the temperature extremes, with maximum deviation of less than 2%. Figure 2 shows that the linear model represented by Equation (5) would not represent the specific heat very well over the wide temperature range required for simulating graphite oxidation.

Comparisons between the reported and the fitted values for carbon dioxide are presented in Figures 3 and 4. The results are similar to, but slightly worse than, those presented previously for oxygen. The maximum deviation between the reported and fitted specific internal energy values was 2.2%. The maximum deviation between the reported and fitted specific heat values was 7%. In both cases, the maximum deviation occurred at 250 K.

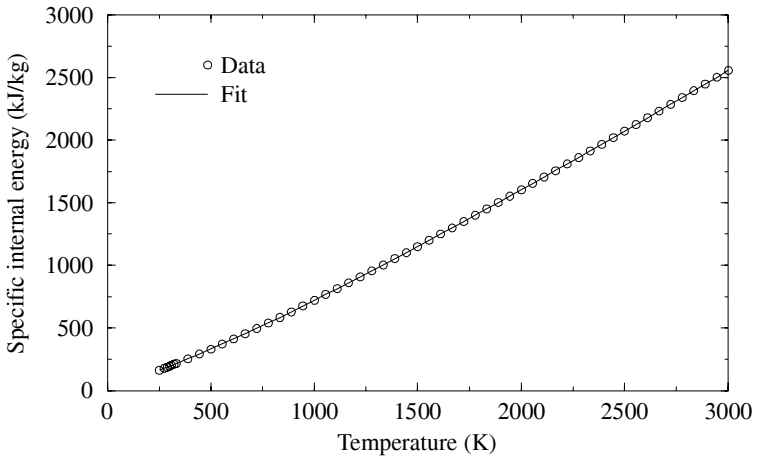

Figure 1. Oxygen specific internal energy as a function of temperature.

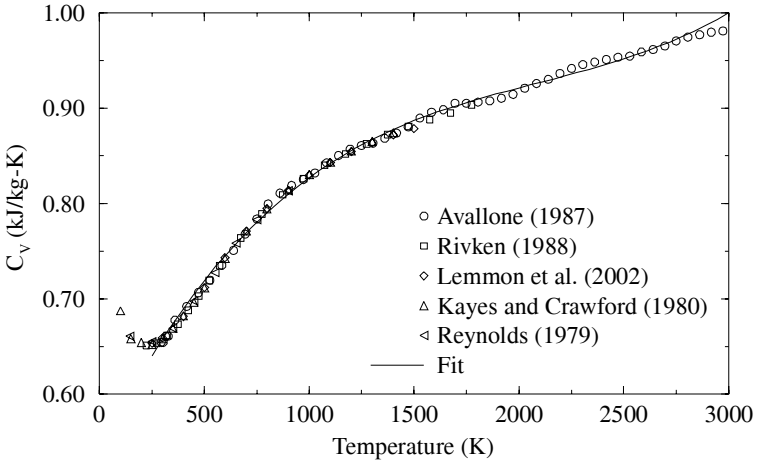

Figure 2. Oxygen specific heat capacity at constant volume as a function of temperature.

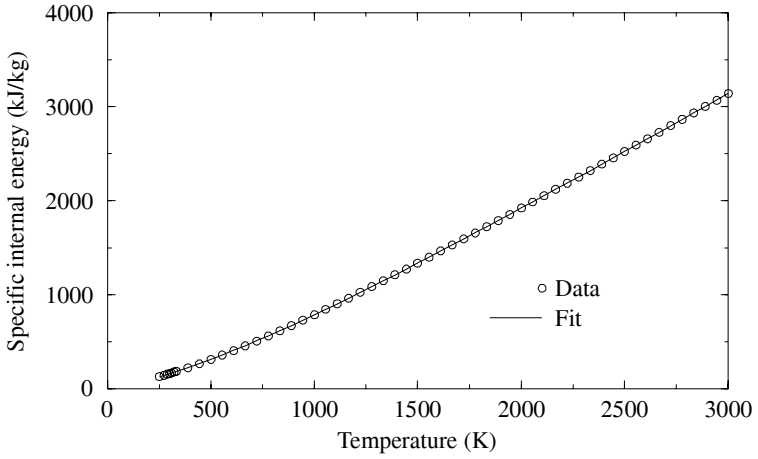

Figure 3. Carbon dioxide specific internal energy as a function of temperature.

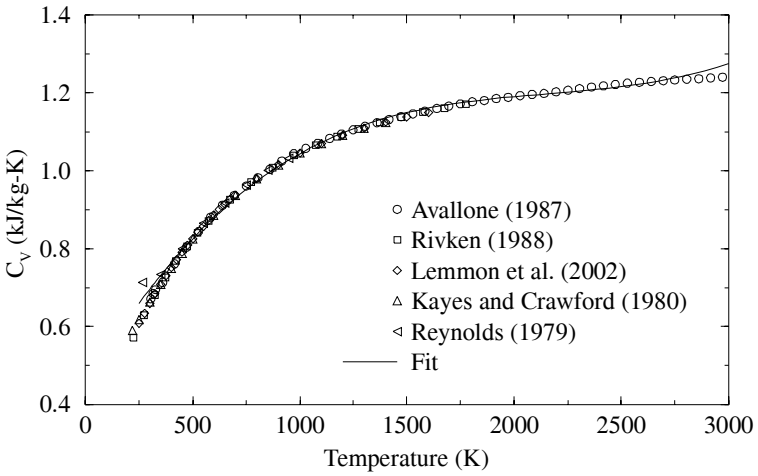

Figure 4. Carbon dioxide specific heat capacity at constant volume as a function of temperature.

Comparisons between the reported and the fitted values for carbon monoxide are presented in Figures 5 and 6. Figure 6 shows a discrepancy in the reported values for the specific heat for carbon monoxide between Lemmon et al. (2002) and the other sources of data. The values of Avallone (1987) and Rivken (1988) were consistent with other references, such as Daubert et al. (2000) and Cambel and Jennings (1958), and thus were used in the least-squares method. The comparison between the results reported by Avallone (1987) and Rivken (1988) and the fitted results were generally similar to, but slightly worse than, those described previously for oxygen. The maximum deviation between the reported and fitted specific internal energy values was 1.2%. The maximum deviation between the reported and fitted specific heat values was 7%. In both cases, the maximum deviation occurred at 250 K.

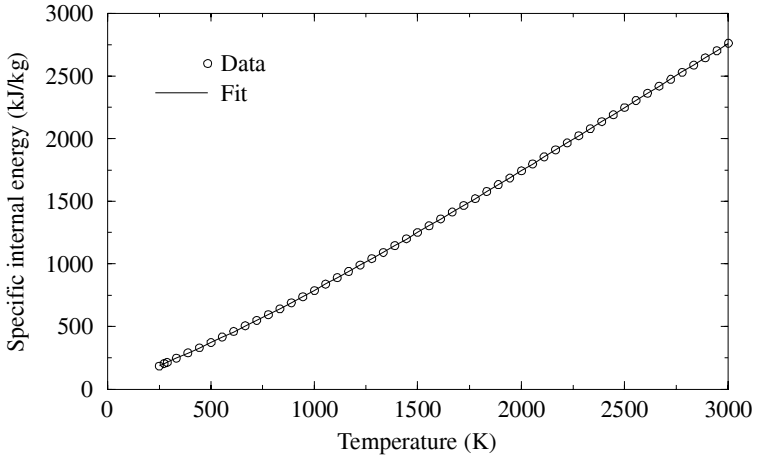

Figure 5. Carbon monoxide specific internal energy as a function of temperature.

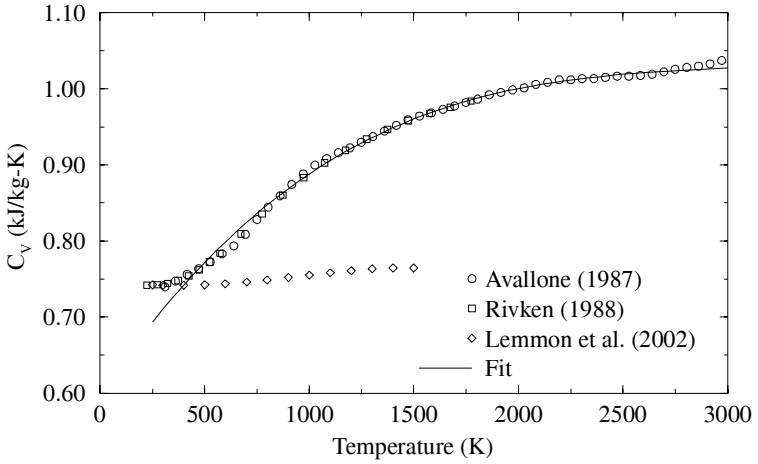

Figure 6. Carbon monoxide specific heat capacity at constant volume as a function of temperature.

Another fourth-order least-squares fit was generated for carbon monoxide in which $C_{o,ni}$ was forced to be 2.5 $R_{o,ni}$ based on kinetic theory. The results of this new fit are presented in Figure 7. A comparison of Figures 6 and 7 reveals that the new fit was better near 250 K, but was significantly worse near 500 K and above 2500 K. Since the higher temperature region is of more concern for graphite oxidation, the original least-squares fit, with the values presented in Table 2, was implemented in the code.

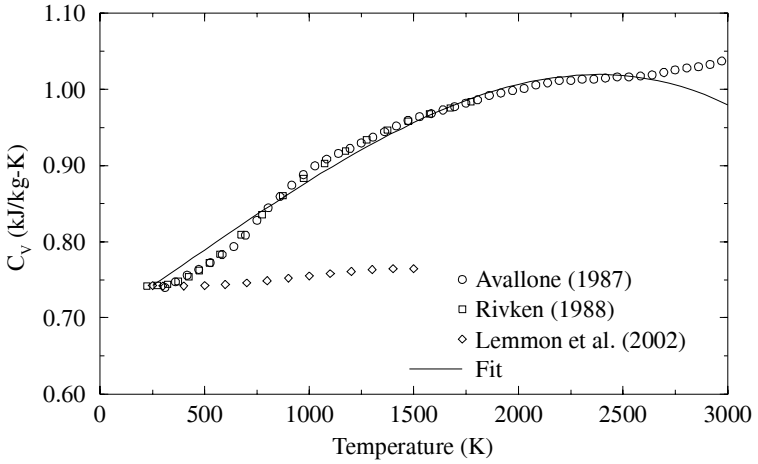

Figure 7. Carbon monoxide specific heat capacity at constant volume with the linear coefficient based on kinetic theory.

Equation (6) was implemented for all of the noncondensable gases in the code, including previously modeled gases such as helium and nitrogen. The coefficients $E_{o,ni}$ and $F_{o,ni}$ were set to zero for the previously modeled gases since new least squares fits for these gases were not generated during this task. Thus, Equation (6) reduces to Equation (2) for the previously modeled gases and the revised code will produce identical results to those obtained previously. The more generalized form of Equation (6) will allow a more accurate representation of the high-temperature range for the previously modeled gases if new fits are generated in the future.

An extrapolation of Figures 2 and 4 indicates that the specific heat capacity at constant volume obtained by differentiating Equation (6) would eventually become too large if extrapolated to too high of a temperature. For example, using the values from Table 1 for carbon dioxide yields a

specific heat capacity at 5000 K that is more than two times the value at 3000 K, which significantly exceeds the value expected by extrapolating the curve of Avallone (1987). If the fit illustrated in Figure 7 had been used, the specific heat capacity for carbon monoxide would have become negative near 5000 K. In order to prevent grossly unphysical results at extremely high temperatures, the specific heat capacity was set to a constant value based on the computed value at 4000 K. Thus, at very high temperatures,

$$C_v\big|_{T=4000} = C_{o,ni} + D_{o,ni}(4000 - T_o) + E_{o,ni}(4000 - T_o)^2 + F_{o,ni}(4000 - T_o)^3 \qquad (7)$$

and

$$U_{ni} = U\big|_{T=4000} + C_v\big|_{T=4000}(T - 4000) \qquad \text{for } T > 4000 \text{ K} \qquad (8)$$

where $U\big|_{T=4000}$ is evaluated from Equation (6). Although somewhat arbitrary, the value of 4000 K prevents the specific heat from exceeding the maximum values shown in the figures by more than 33%.

Thermal Conductivity

RELAP5-3D assumes that the thermal conductivity of a noncondensable gas, k, can be represented as

$$k = AT^B \qquad (9)$$

where k is in W/m-K and T is the temperature in degrees K.

The values for A and B for most of the noncondensable gases currently modeled in RELAP-3D are given in Table 12-1 of the MATPRO library used in the SCDAP/RELAP5-3D computer code (SCDAP/RELAP5-3D Development Team 2002). However, the database used in the development of the MATPRO constants for oxygen, carbon dioxide, and carbon monoxide was limited to 700 K, which is considerably below the temperatures of interest relative to graphite oxidation. Consequently, several other sources of data were evaluated for the oxygen, carbon dioxide, and carbon monoxide gases. These sources of data include Lemmon et al. (2002), Daubert et al. (2000), and Kayes and Crawford (1980). Thermal conductivities from the various references are compared in Figures 8 through 10. All of the references were in reasonable agreement for oxygen, as the deviations between references were generally less than 10% of the values from Lemmon et al. (2002). For carbon dioxide and carbon monoxide, however, the values from MATPRO were more than 30% higher than from the other references at 1500 K. This is not entirely unexpected because of the rather limited temperature range in the MATPRO database.

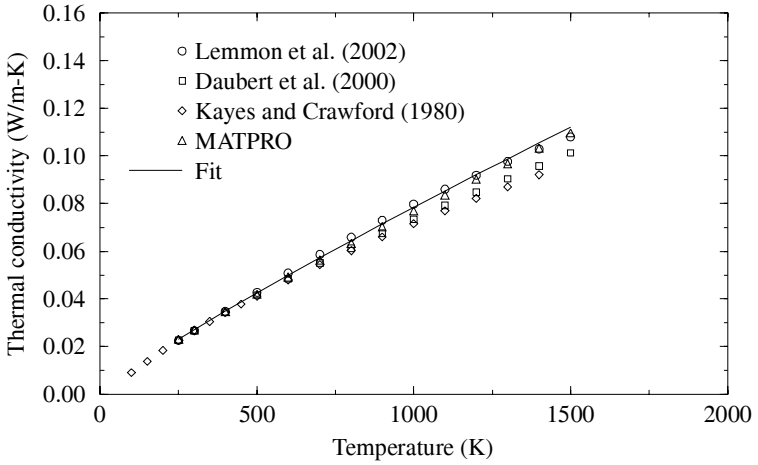

Figure 8. Thermal conductivity of oxygen as a function of temperature.

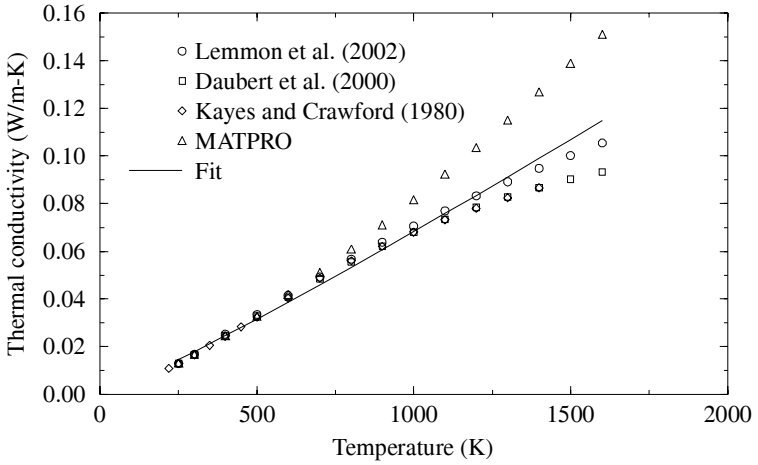

Figure 9. Thermal conductivity of carbon dioxide as a function of temperature.

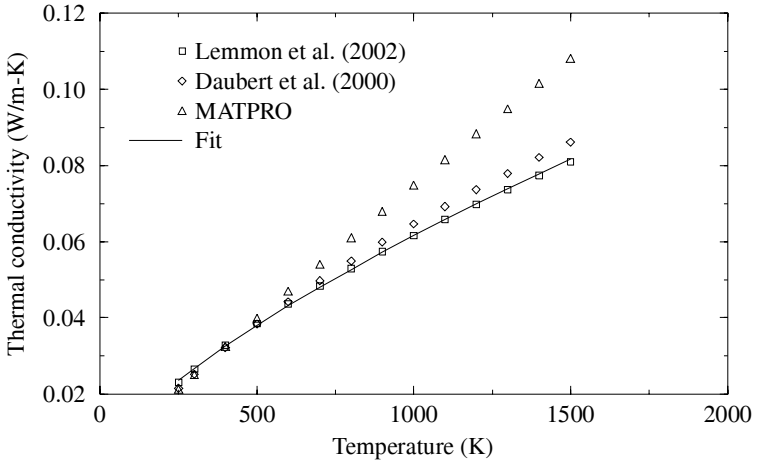

Figure 10. Thermal conductivity of carbon monoxide as a function of temperature.

Based on the results shown in Figures 8 through 10, data from Lemmon et al. (2002) were used to determine the values of A and B using the method of least squares. The results of the least-squares fit are presented in Table 3. The results of the least squares fit are also shown in Figures 8 through 10. The least-squares fit matched the values from Lemmon et al. (2002) to within 4%

for oxygen, 12% for carbon dioxide, and 2% for carbon monoxide over the range shown in the figures.

Table 3. Thermal conductivity constants.

Gas species	A ($W/m\text{-}K^{1+B}$)	B
Oxygen	1.766e-4	0.8824
Carbon dioxide	3.110e-5	1.1136
Carbon monoxide	5.050e-4	0.6954

Viscosity

RELAP5-3D assumes that the viscosity, μ, of a noncondensable gas can be represented as

$$\mu = \frac{AT^{1.5}}{T + B} \tag{10}$$

where μ is in kg/m-s, T is the temperature in degrees K, and A and B are constants.

The values for A and B were determined using the method of least squares. Because the form of Equation (10) differs from that typically used for least-squares fitting, additional details are provided below. The coefficients A and B are chosen to minimize the function f

$$f(A,B) = \sum_i \left[y_i - \frac{AT_i^{1.5}}{T_i + B} \right]^2 \tag{11}$$

where y_i is the value of the viscosity corresponding to a temperature T_i. Taking the partial derivative of f with respect to A, setting it equal to zero, and solving for A yields

$$A = \frac{\sum_i \frac{y_i T_i^{1.5}}{T_i + B}}{\sum_i \frac{T_i^3}{(T_i + B)^2}} \tag{12}$$

Because the partial derivative with respect to B does not lend itself to algebraic solution, an iterative technique was employed. Specifically, a value of B was assumed, Equation (12) was used to calculate the optimal value of A consistent with the assumed value of B, and then the sum in Equation (11) was determined. The value of B was then varied by hand until the sum in Equation (11) was minimized.

Table 4 shows the optimal values of A and B that were obtained fitting the data of Lemmon et al. (2002). The results of the fitting process are compared with data from Lemmon et al. (2002) and Daubert et al. (2000) in Figures 11 through 13. Figures 11 and 12 also contain values from Kayes and Crawford (1980). The viscosity data from the various references were consistent and agreed to within 5% over the temperature ranges presented in the figures.

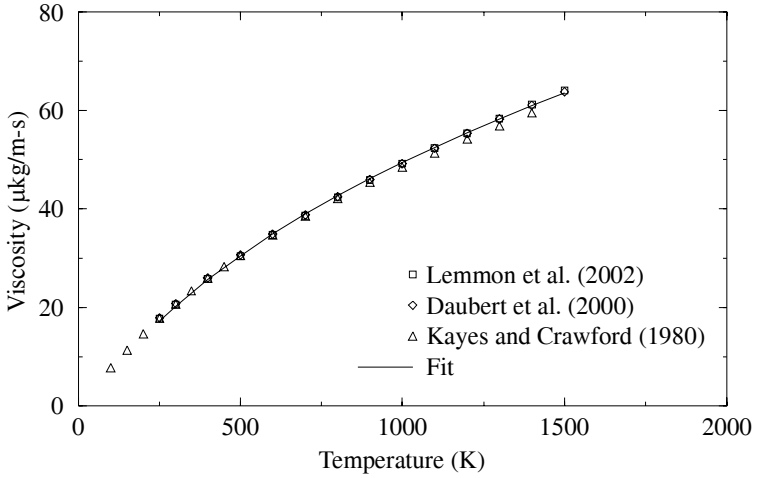

Figure 11. Viscosity of oxygen as a function of temperature.

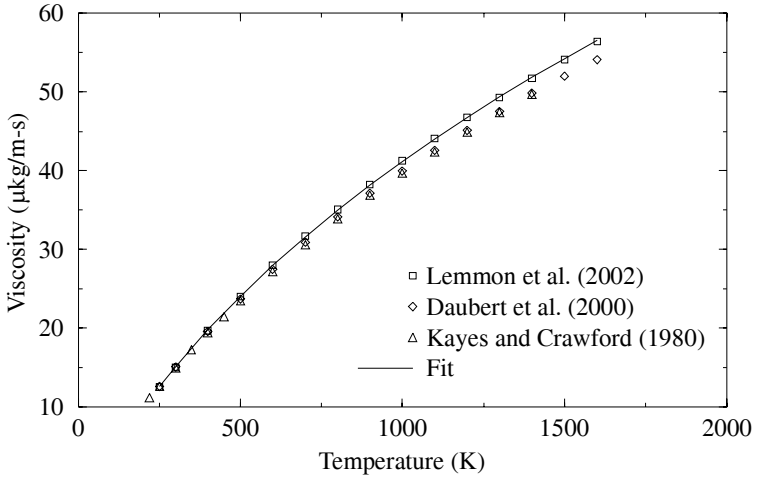

Figure 12. Viscosity of carbon dioxide as a function of temperature.

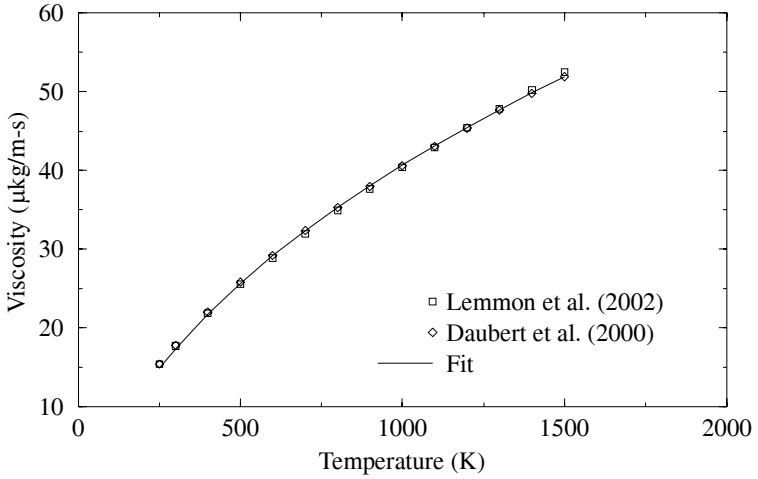

Figure 13. Viscosity of carbon monoxide as a function of temperature.

The least-squares fit matched the values from Lemmon et al. (2002) to within 3% for oxygen, 1% for carbon dioxide, and 4% for carbon monoxide over the ranges shown in the figures.

Table 4. Viscosity constants.

Gas species	A (kg/m-s-K$^{0.5}$)	B (K)
Oxygen	1.826e-6	169
Carbon dioxide	1.651e-6	268
Carbon monoxide	1.463e-6	138

Diffusion Parameters

The presence of a noncondensable gas can significantly affect the heat transfer coefficient during condensation. RELAP5-3D represents this effect by simulating the diffusion of the noncondensable gas from a homogeneous steam/noncondensable mixture to the surface of a water film. The RELAP5-3D model is based on the diffusion coefficient given by Equation (11.4.4) of Reid et al. (1987)

$$D_{AB} = \frac{0.00143T^{1.75}}{PM_{AB}^{1/2}\left[\left(\sum_v\right)_A^{1/3} + \left(\sum_v\right)_B^{1/3}\right]^2} \tag{13}$$

where

D_{AB} = binary diffusion coefficient (cm^2/s)
T = temperature (K)
P = pressure (bar)
M_A, M_B = molecular weights of A and B (g/mole) and
$M_{AB} = 2/\left[(1/M_A) + (1/M_B)\right]$
$\sum_v$ = atomic diffusion volume given in Table 11-1 of Reid et al. (1987).

Converting to the units used by RELAP5-3D yields

$$D_{AB} = \frac{D_c T^{1.75}}{P} \tag{14}$$

where

D_{AB} = binary diffusion coefficient (m^2/s)
P = pressure (Pa)

and

$$D_C = \frac{\frac{0.0143}{\sqrt{2}}\left[\frac{1}{M_A} + \frac{1}{M_B}\right]^{1/2}}{\left[\left(\sum_v\right)_A^{1/3} + \left(\sum_v\right)_B^{1/3}\right]^2} \quad \frac{m^2\ Pa}{s\ K^{1.75}} \tag{15}$$

The constant D_C was determined for each noncondensable gas using the values given in Table 5, a molecular weight of 18.016 (Zucrow and Hoffman (1976)) for water, and an atomic diffusion volume of 13.1 for water (Reid at al. 1987).

Table 5. Diffusion parameters.

Gas species	Molecular weight	$\sum_v$	D_C m^2-Pa/s-$K^{1.75}$
Oxygen	32.000	16.3	1.2441×10^{-4}
Carbon dioxide	44.010	26.9	9.8678×10^{-5}
Carbon monoxide	28.010	18.0	1.2323×10^{-4}

CONCLUSIONS

The code's original noncondensable gas model assumed that the specific internal energy was at most a quadratic function of temperature. Based on the results shown in Figures 2, 4, and 6, the quadratic assumption is reasonable for the temperature range between 250 and 700 K, but is not sufficiently accurate when the temperatures are extended to near 2000 K. Thus, the quadratic model was not adequate to represent graphite oxidation in a very-high temperature gas reactor and was replaced by a more general, fourth-order polynomial.

The fitted results for the three new noncondensable gases are in reasonable agreement with values reported from the literature for specific internal energy and specific heat capacity at constant volume for temperatures between 250 and 3000 K. The maximum deviation between the calculated and reported internal values was 2.2% for the specific internal energy and 7% for the specific heat capacity at constant volume. The maximum deviations occurred at the temperature extremes, either at 250 K or 3000 K.

The fitted results for the transport properties were also in reasonable agreement with values from the literature for temperature between 250 and 1500 K. The maximum fitting errors were less than 4% for oxygen and carbon monoxide. The maximum fitting for the viscosity of carbon dioxide was 4%. The maximum error was larger (12%) for the thermal conductivity of carbon dioxide, but the new fit represents a significant improvement compared to the correlation used in MATPRO at temperatures above 1000 K. The fitted results are generally within the scatter of values from different references.

ACKNOWLEDGMENTS

This work was supported through the Department of Energy's International Nuclear Energy Research Initiative Project NE-INERI-2002-001 under DOE Idaho Operations Office Contract DE-AC07-99ID13727.

REFERENCES

Avallone, E. A, 1987, Marks' Standard Handbook for Mechanical Engineers, Ninth Edition, McGraw-Hill Book Company, New York.

Cambel, A. B. and B. H. Jennings, 1958, Gas Dynamics, McGraw-Hill Book Company, New York.

Carlson, K. E., R. A. Riemke, S. Z. Rouhani, R. W. Shumway, and W. L. Weaver, 1990, "RELAP5/MOD3 Code Manual Volume III: Developmental Assessment Problems (DRAFT)," NUREG/CR-5535 EGG-2596, June.

Daubert, T. E., R. P. Danner, H. M. Sibul, C. C. Stebbins, R. L. Rowley, W. V. Wilding, J. L. Oscarson, M. E. Adams, T. L. Marshall, and N. A. Zundel, 2000, "Physical and Thermodynamic Properties of Pure Chemicals," DIPPR Project 801 Evaluated Process Design Data, American Institue of Chemical Engineers and Design Institute for Physical Property Data.

Oh, C. H., L. J. Siefken, R. Moore, C. Davis, J. Lee, W. Martin, J. Holloway, H. C. No, J. H. Kim, and G. C. Park, 2002, "Development of Safety Analysis Codes and Experimental Validation for a Very High Temperature Gas-Cooled Reactor," International Nuclear Energy Research Initiative Proposal, Program Announcement, NE-INERI-2002-001.

RELAP5-3D Development Team, 2002, "RELAP5-3D Code Manual" INEEL-EXT-98-00834, Revision 2.0, July.

SCDAP-RELAP5-3D Development Team, 2002, "Volume 4: MATPRO—A Library of Materials Properties for Light-Water-Reactor Accident Analysis," INEEL-EXT-02-00589, May.

Kays, W. M. and M. E. Crawford, 1980, Convective Heat and Mass Transfer, Second Edition, McGraw-Hill Book Company, New York.

Lemmon, E. W., M. O. McLinden, and M. L. Huber, 2002, REFPROP Reference Fluid Thermodynamic and Transport Properties, NIST Standard Reference Database 23, Version 7.0 Beta Version, National Institute of Standards and Technology.

Reid, R. C., J. M Prausnitz and B. E. Poling, 1987, The Properties of Gases and Liquids, Fourth Edition, McGraw-Hill Book Company, New York.

Reid, R. C., J. M Prausnitz and T. K. Sherwood, 1977, The Properties of Gases and Liquids, Third Edition, McGraw-Hill Book Company, New York.

Reynolds, W. C., 1979, Thermodynamic Properties in SI, Stanford University.

Rivken, S. L, 1988, Thermodynamic Properties of Gases, Fourth Edition (Revised), Hemisphere Publishing Corporation.

Shumway, R. W., 1995, "Assessment of RELAP5/MOD3.2 Condensation Models," Developmental Assessment Test Report, R5M3DA-004.

Siefken, L. J., E. W. Coryell, and E. A. Harvego, 2002, "Conceptual Designs of Models for the Transient Analysis of Pebble Bed High Temperature Gas-Cooled Reactors," INEEL/INT-02-00154, January.

Zucrow, M. J. and J. D. Hoffman, 1976, Gas Dynamics, Volume 1, John Wiley and Sons, New York.